THE JOURNAL OF BIOLOGICAL CHEMISTRY VOL. 291, NO. 7, pp. 3184–3196, February 12, 2016

Low Level Pro-inflammatory Cytokines Decrease Connexin36 Gap Junction Coupling in Mouse and Human Islets through Nitric Oxide-mediated Protein Kinase Cδ*

Received for publication, July 17, 2015, and in revised form, December 7, 2015 Published, JBC Papers in Press, December 14, 2015, DOI 10.1074/jbc.M115.679506

Nikki L. Farnsworth[‡§], Rachelle L. Walter[§], Alireza Hemmati[§], Matthew J. Westacott[§], and Richard K. P. Benninger[‡§1]

From the [‡]Barbara Davis Center for Childhood Diabetes, [§]Department of Bioengineering, University of Colorado, Anschutz Medical Campus, Aurora, Colorado 80045

Pro-inflammatory cytokines contribute to the decline in islet function during the development of diabetes. Cytokines can disrupt insulin secretion and calcium dynamics; however, the mechanisms underlying this are poorly understood. Connexin36 gap junctions coordinate glucose-induced calcium oscillations and pulsatile insulin secretion across the islet. Loss of gap junction coupling disrupts these dynamics, similar to that observed during the development of diabetes. This study investigates the mechanisms by which pro-inflammatory cytokines mediate gap junction coupling. Specifically, as cytokine-induced NO can activate PKCδ, we aimed to understand the role of PKCδ in modulating cytokine-induced changes in gap junction coupling. Isolated mouse and human islets were treated with varying levels of a cytokine mixture containing TNF-α, IL-1β, and IFN-γ. Islet dysfunction was measured by insulin secretion, calcium dynamics, and gap junction coupling. Modulators of PKCδ and NO were applied to determine their respective roles in modulating gap junction coupling. High levels of cytokines caused cell death and decreased insulin secretion. Low levels of cytokine treatment disrupted calcium dynamics and decreased gap junction coupling, in the absence of disruptions to insulin secretion. Decreases in gap junction coupling were dependent on NO-regulated PKCδ, and altered membrane organization of connexin36. This study defines several mechanisms underlying the disruption to gap junction coupling under conditions associated with the development of diabetes. These mechanisms will allow for greater understanding of islet dysfunction and suggest ways to ameliorate this dysfunction during the development of diabetes.

Diabetes is characterized by a progressive decrease in function and mass of β-cells, which comprise the majority of cells in the islets of Langerhans (1). Pro-inflammatory cytokines have been implicated as mediators of β-cell death in both type 1 diabetes (T1D)[2] and type 2 diabetes (T2D) (2–4). However, pro-inflammatory cytokines also play a role in causing β-cell dysfunction early in disease progression (3, 5). In T1D, high levels of pro-inflammatory cytokines, including tumor necrosis factor-α (TNF-α), interleukin-1β (IL-1β), and interferon γ (IFN-γ), are released by immune cells, such as $CD4^+$ and $CD8^+$ T-cells and macrophages, which infiltrate the pancreas (3, 6). In T2D, adipocyte stress resulting from obesity can lead to secretion of low levels of circulating TNF-α from activated macrophages in adipose tissue; whereas elevated free fatty acids and/or hyperglycemia can also lead to local release of IL-1β in the islets (4, 7). Although the mechanisms of cytokine-induced cell death in diabetes are well characterized, cytokine-induced islet dysfunction is poorly understood.

In vitro, the pro-inflammatory cytokines TNF-α, IL-1β, and IFN-γ work synergistically (8) to induce islet dysfunction and disrupt insulin secretion (9, 10). The effect of pro-inflammatory cytokines on the β-cell is thought to be mediated in part by the generation of nitric oxide (NO) (9, 11), where NO production has also been shown to modulate intracellular calcium ($[Ca^{2+}]_i$) in rat islets (12). In the β-cell, glucose-stimulated $[Ca^{2+}]_i$ influx initiates insulin release. An initial pulse of $[Ca^{2+}]_i$ stimulates a pulse of insulin (first phase insulin release) and subsequent $[Ca^{2+}]_i$ oscillations stimulate prolonged insulin secretion (13). These dynamics have been shown to be important for hepatic insulin signaling (14). Pro-inflammatory cytokines have been shown to disrupt $[Ca^{2+}]$ oscillations (10), which has been attributed to altered endoplasmic reticulum uptake (15) and can impact $[Ca^{2+}]_i$ dynamics. Similar disruptions to $[Ca^{2+}]_i$ oscillations have been observed in islets from a diabetic mouse model (16). As $[Ca^{2+}]_i$ regulates glucose-stimulated insulin secretion, altered $[Ca^{2+}]_i$ may partially mediate cytokine-induced changes in insulin secretion (17).

Connexin36 (Cx36) gap junctions strongly regulate $[Ca^{2+}]_i$ dynamics within the islet (18) by coordinating glucose-induced membrane depolarization. Under stimulatory conditions, gap junction coupling coordinates $[Ca^{2+}]_i$ oscillations across the

* This work was supported, in whole or in part, by National Institutes of Health Grants R00 DK085145, R01 DK102950, and R01 DK106412, and Juvenile Diabetes Research Foundation Grant 5-CDA-2014-198-A-N (to R. K. P. B.), National Institutes of Health Grant F32 DK102276 and a Blum-Kovler Scholarship (to N. L. F.), and University of Colorado internal funds. Imaging experiments performed in the University of Colorado Anschutz Medical Campus Advance Light Microscopy Core were supported in part by National Institutes of Health Grants UL1 TR001082 and P30 NS048154. Islet isolation performed in the Barbara Davis Center Islet Core was supported in part by P30 DK057516. Authors declare no conflict of interest.

[1] To whom correspondence should be addressed: 1775 Aurora Ct., M20-4306D, Mail Stop B140, University of Colorado Anschutz Medical campus, Aurora, CO 80045. Tel.: 303-724-6388; Fax: 303-724-5800; E-mail: richard.benninger@ucdenver.edu.

[2] The abbreviations used are: T1D, type 1 diabetes; T2D, type 2 diabetes; $[Ca^{2+}]_i$, intracellular calcium; Cx36, connexin36; C57BL/6, C57BL/6NHsd; SNAP, *S*-nitroso-*N*-acetyl-DL-penicillamine; DEANO, diethylamine NONOate; L-NAME, L-NG-nitroarginine methyl ester; cPTIO, 2-(4-carboxyphenyl)-4,4,5,5-tetramethylimidazoline-1-oxyl-3-oxide potassium salt; CIP, calf intestinal phosphatase; RCC, relative cytokine concentration.

islet, first phase insulin release, and second phase insulin pulses (19). Altered Cx36 gap junction coupling in pancreatic islets can cause disruptions to $[Ca^{2+}]_i$ signaling and insulin secretion dynamics (18, 20). These dynamics, specifically first phase insulin release and pulsatile insulin release, are similarly disrupted in states of pre-diabetes in animal models and humans (21–23). This suggests that disruptions to gap junction coupling occur under these pre-diabetic and diabetic conditions. Recent studies have shown that Cx36 gap junction coupling is decreased in high-fat diet fed mice (24), which suggests a role for altered coupling in the development of disease. Furthermore, *in vitro* studies have shown that hyperglycemia (25) and hyperlipidemia (26, 27), conditions that stimulate high levels of cytokine production from β-cells (28, 29), reduce Cx36 gap junction coupling. Therefore, changes in Cx36 gap junction coupling could underlie a component of cytokine-induced islet dysfunction in diabetes. Based on the results of these previous studies, we aim to investigate if pro-inflammatory cytokines decrease Cx36 gap junction coupling in the islet and the mechanisms involved in this disruption.

Changes in Cx36 gap junction coupling have been shown to be protective against cytokine-induced damage in INS-1E cells (30) and against apoptosis in mouse islets (31). Despite this protective mechanism and the importance of Cx36 in regulating insulin release, the regulation of Cx36 gap junction coupling in the islet is poorly understood (32). Gap junctions are regulated by protein kinases in several tissues (33). For example, protein kinase A decreases Cx36 gap junction coupling in AII amacrine cells (34), and PKC decreases Cx43 channel conductance in rat epithelial cells (35). Cytokine-induced NO production activates protein kinase Cδ (PKCδ) in cardiomyocytes (36) and PKCδ is activated by pro-inflammatory cytokines in the islet (37). Furthermore, deletion of PKCδ in mice has been shown to protect β-cells from cytokine-induced death (38). Therefore NO-activated PKCδ may participate in the regulation of Cx36 under pro-inflammatory conditions.

The goal of this study is to quantify changes in Cx36 gap junction coupling with varying levels of pro-inflammatory cytokines and determine the role of PKCδ in modulating cytokine-induced changes in gap junction coupling. Several studies have shown islet dysfunction and extensive cell death with high levels of pro-inflammatory cytokines, but lower levels of inflammation, associated with earlier stages of diabetes progression, have not been studied. Therefore this study aims to investigate islet dysfunction over a range of cytokine levels to determine the mechanisms for altered insulin secretion, altered $[Ca^{2+}]_i$ signaling dynamics, and disruption to Cx36 gap junction coupling. We specifically test whether low levels of pro-inflammatory cytokines decrease gap junction coupling through NO-regulated PKC_δ.

Materials and Methods

Animal Care—All experiments using mice were performed in compliance with the guidelines and relevant laws set by the University of Colorado, and were approved by the University of Colorado Institutional Animal Care and Use Committee. Mice were given food and water *ad libitum* and were housed in a temperature and light controlled facility with 12-h light-dark cycles. A total of 110 C57BL/6NHsd (C57BL/6) mice were used.

Islet Isolation, Culture, and Cytokine Treatment—For all experiments, islets were isolated from 8–16-week-old C57BL/6 mice as previously described (39, 40). Islets were cultured overnight in RPMI medium 1640 (Life Technologies) with 10% FBS, 11 mM glucose, 100 units/ml of penicillin, and 100 μg/ml of streptomycin at 37 °C under humidified 5% CO_2 before commencing experiments. Human islets were received from the Integrated Islet Distribution Program (donor IDs: AAEZ340, AAJF122, ABAF490, ABCQ166, ABD1375, ABEI419, ABFV041, ABGK387A, ABHC283, ABJR111, and ABJ5204) with a median viability of 90% and an average stimulation index (fold-increase insulin secretion from 2 to 20 mM glucose) of 2.5 for all donors, and were cultured overnight in CMRL medium 1066 (Fisher Scientific) before commencing experiments. Islets were treated for 1 h, 24 h, or 30 min in RPMI medium with 0, 0.001, 0.01, 0.1, or 1 times dilutions of a cytokine mixture (termed "relative cytokine concentration" or RCC) consisting of 10 ng/ml of recombinant mouse tumor necrosis factor-α (TNF-α, R&D Systems, Minneapolis, MN), 5 ng/ml of recombinant mouse interleukin-1β (IL-1β, R&D Systems), and 100 ng/ml of recombinant mouse interferon-γ (IFN-γ, R&D Systems) (10, 30). Islets were also treated with individual or combinations of two cytokines at 0.1 RCC for 24 h.

Intracellular Ca^{2+} Imaging and Analysis—Islets were incubated with 4 μM Fluo-4 AM for 2 h at room temperature in imaging buffer (125 mM NaCl, 5.7 mM KCl, 2.5 mM $CaCl_2$, 1.2 mM $MgCl_2$, 10 mM HEPES, 0.1% bovine serum albumin (BSA), and 2 mM glucose). Islets were imaged in a polymdimethylsiloxane microfluidic device (41) maintained at 37 °C with an Eclipse-Ti wide field microscope (Nikon) and a ×20 0.75 NA Plan Apo objective. Images were acquired at 1 frame/s for either 5 min after stimulation with 11 mM glucose for 10 min, or continuously for 20 or 50 min from low to high glucose. Fluo-4 was imaged using a 490/40-nm band-pass excitation filter and a 525/36-nm band-pass emission filter (Chroma). Islets were treated for 24 h, 1 h immediately prior to imaging, or 30 min while imaging continuously. The percentage islet area synchronized was determined as previously described (42) over 300- or 400-s intervals. Peak $[Ca^{2+}]_i$ was calculated as the difference in Fluo-4 AM intensity averaged over the entire islet at the peak and trough of each glucose-induced oscillation, normalized to the average intensity at the trough, and averaged over 300- or 400-s intervals.

Islet Viability—Islets were incubated with a near IR fluorescent reactive dye (Life Technologies) diluted 1:1000 in imaging buffer for 30 min at room temperature. Islets were imaged on a Zeiss LSM 510 Meta confocal microscope (Zeiss, Thornwood, NY) with a ×40 1.2NA water immersion objective. The dye was excited with a 633-nm helium-neon laser with a UV/488/543/633-nm dichroic beam splitter and images for live/dead cells were collected with a 650–710 nm band-pass emission filter. Viability was calculated from manual counts of live and dead cells averaged over 3 images of increasing depth in each islet.

Insulin Secretion ELISA—Insulin secretion samples were collected by incubating ~10 islets in 500 μl of Krebs-Ringer buffer with 2 mM glucose for 1 h, followed by 1 h at 2 mM glucose, 20

mM glucose, or 20 mM glucose plus 20 mM KCl. Supernatant and islet lysate were collected for analysis of insulin secretion and content, respectively. Islets were lysed by freezing in 2% Triton X-100 in deionized water. Insulin was measured with a mouse ultrasensitive insulin ELISA kit (ALPCO) per the manufacturer's instructions, and is reported as secretion (supernatant) normalized to content (lysate) for each sample.

Fluorescence Recovery after Photobleaching (FRAP)—FRAP was used to quantify the extent of Cx36 gap junction coupling, as previously described (43). Briefly, islets were cultured in MatTek dishes (MatTek Corp., Ashland, MA) coated with Cell-Tak (BD Biosciences, San Jose, CA) and stained with 12.5 μM rhodamine 123 (Sigma) for 30 min at 37 °C. Islets were imaged on a Zeiss LSM 510 Meta confocal microscope with a ×40 1.2NA water immersion objective. Rh123 was excited with an argon laser at 488 nm and images were collected with a 488-nm narrow band-pass dichroic beam splitter, 490-nm long pass secondary dichroic beam splitter, and a 505-nm long pass emission filter. Half of the islet area was photobleached for 235.5 s at 316.05 milliwatt/cm^2 and the fluorescence recovery was measured in the bleached area. Recovery rates were calculated from the inverse exponential fluorescence recovery curve for either the entire bleached area or for individual cells in the bleached area.

NO and PKCδ Regulation of Cx36 Gap Junction Coupling—To determine the role of PKCδ in regulating gap junction coupling, islets were cultured with the following treatments: 300 nM PKCδ-specific activator phorbol 12-myristate 13-acetate (PMA, Sigma), or 0.1 RCC with 1 μM of the PKCδ specific inhibitor rottlerin (Sigma) for 1 h. To determine the role of NO in regulating gap junction coupling, islets were cultured with the following treatments: 5 mM of the NO donor molecule *S*-nitroso-*N*-acetyl-DL-penicillamine (SNAP, Sigma), 100 mM of the nitric oxide donor molecule diethylamine NONOate (DEANO, Calbiochem), 1 mM of the nitric-oxide synthase inhibitor L-NG-nitroarginine methyl ester (L-NAME, Santa Cruz Biotechnology), or 200 μM of the nitric oxide scavenging molecule 2-(4-carboxyphenyl)-4,4,5,5-tetramethylimidazoline-1-oxyl-3-oxide potassium salt (cPTIO, Sigma), each for 1 h.

Western Blot Analysis—For analysis of PKCδ activation by tyrosine phosphorylation, mouse islets were cultured for 24 h with treatments as previously described. Islets (100 per treatment) were washed once in PBS and lysed by sonication for 30 s in 50 μl of lysis buffer containing 100 mM NaCl, 50 mM Tris-HCl, 10 mM $MgCl_2$, and 1 mM dithiothreitol with a mixture of protease inhibitors (Roche Diagnostics). Protein content was measured using the Pierce BCA Protein Assay Kit (Thermo Scientific, Rockford, IL) per the manufacturer's instructions. Non-phosphorylated PKCδ controls were generated by incubating 5 μg of protein from SNAP-treated samples with 5 units of calf intestinal phosphatase (CIP, New England Biolabs, Ipswitch, MA) in 25 μl of lysis buffer for 1 h at 37 °C. Samples were run on 15% TGX pre-cast gels (Bio-Rad) and transferred to a PVDF membrane (GE Life Sciences). The membrane was blocked in 5% dry milk (Fisher Scientific) in PBS with 1% Tween 20 (Sigma) (PBST) for >2 h, then stained with a rabbit anti-PKCδ primary antibody, which binds to the activated (phosphorylated) form of PKCδ (Y311, Cell Signaling Technologies) diluted 1:1,000 or a monoclonal mouse anti-α-tubulin primary antibody (NB100–690SS, Novus Biologicals) diluted 1:5,000 at 4 °C for >16 h. The membrane was then stained with either a goat anti-rabbit horseradish peroxidase (HRP)-conjugated secondary antibody (111-035-003, Jackson ImmunoResearch) diluted 1:10,000 in PBST with 5% dry milk; or a goat anti-mouse HRP-conjugated secondary antibody (A4416, Sigma) diluted 1:10,000 for 2 h at room temperature. The membranes were incubated with Amersham Biosciences ECL Prime (GE Life Sciences) for 5 min in the dark, and then visualized. Protein quantification was performed with ImageJ (NIH). Background was subtracted from the measured intensity for each sample. Total activated PKCδ was normalized to α-tubulin for each sample.

For analysis of changes in Cx36 protein in the cell membrane and cytosol, islets (100 per treatment) were treated for 24 or 1 h as previously described. Islets were lysed by sonication as previously described, and incubated for 30 min at 4 °C with shaking. Lysate was centrifuged at 500 × *g* for 10 min to remove nuclei, and the supernatant was collected. To fractionate the protein into cytosolic and membrane fractions, samples were centrifuged at 45,000 rpm (~100,000 × *g*) for 1 h at 4 °C. Supernatants were collected, which represents cytosolic protein, and the pellet, which represents membrane protein, was reconstituted in lysis buffer with 1% SDS for 30 min at 4 °C with shaking. Protein from the supernatant and pellet was quantified, separated by electrophoresis, and transferred to a PVDF membrane. The membrane was blocked, and incubated overnight at 4 °C with rabbit anti-Cx36 primary antibody (Abcam, ab48814) diluted 2:1000 in blocking buffer. The blots were incubated with HRP anti-rabbit secondary antibody, followed by ECL prime as previously described, and then visualized. Total protein was subsequently measured after staining for 5 min with Ponceau S (Sigma). Total Cx36 in the supernatant (115 plus 75-kDa bands: trimers and dimers, respectively) and pellet (115-kDa band: trimers) was normalized to total protein for each sample.

Immunofluorescence and Image Analysis—Mouse islets were treated as previously described for 1 or 24 h. Islets were either incubated with 5 μg/ml of FM 4-64FX (Life Technologies) for 1 min on ice prior to fixation, or directly fixed in 8% formalin for 10 min on ice. Islets were cryosectioned (20-μm sections), blocked for 5 min in PBS with 1% BSA, and probed with a rabbit anti-Cx36 primary antibody (36-4600, Invitrogen) diluted 1:50 in PBS with 1% BSA overnight at 4 °C. Islet sections that were not stained with FM 4-64FX were incubated with mouse anti-NCAM primary antibody (Cell Signaling Technology, 3576S) diluted 1:100, as well as rabbit anti-Cx36 primary antibody. Slides were then probed with either Alexa Fluor 488 donkey anti-rabbit secondary antibody (711-545-152, Jackson ImmunoResearch) alone or combined with Alexa Fluor 647 donkey anti-mouse secondary antibody, both diluted 1:500 in PBS with 1% BSA overnight at 4 °C. Slides were imaged on a 510 META laser scanning microscope (Zeiss) with a ×63 1.4 NA oil immersion objective. Alexa Fluor 488 was excited with an Argon laser with a UV/488/543/633-nm beam splitter and images were collected with a 500–530 band pass filter. FM 4-64FX and Alexa 647 were excited at 543 nm with a helium-neon laser with a UV/488/543/633-nm beam splitter and

images were collected with a 650–710-nm band-pass filter. Islets were imaged with a pixel size of diameter 0.087 μm, where 4–7 images per islet were collected at 1-μm increments in depth.

For each image, nuclei were manually counted using ImageJ. Image analysis was performed blinded using custom routines written in MATLAB. Masks were created for fluorescence intensity of Alexa Fluor 488 (Cx36 staining) and FM 4-64FX or NCAM (plasma membrane staining) by determining the average fluorescence intensity values for Cx36 plaques, cytoplasmic membrane, and background signal. Contiguous regions of Cx36-positive staining were automatically identified and plaques that were outside of the membrane mask were removed, ensuring only Cx36 on the cell surface was included in further analysis. Very large objects that were identified by the program but morphologically did not resemble Cx36 plaques were removed from the dataset using 95% confidence intervals about the mean plaque area and were confirmed manually. Additionally, plaques with lengths smaller than the point spread function for the ×63 objective (diameter 0.425 μm, 4.8 pixels), which would represent spurious noise, were automatically removed.

Statistical Analysis—Data represent the average over all mice for each measurement with error bars representing the mean ± S.E. Statistical significance was determined using either an analysis of variance with Tukey's post hoc analysis and $\alpha = 0.05$, or 95% confidence intervals where indicated.

Results

Low Levels of Pro-inflammatory Cytokines Alter $[Ca^{2+}]_i$ Dynamics—To determine the concentration of pro-inflammatory cytokines necessary to cause islet dysfunction, islets were cultured for 24 h with a range of relative cytokine concentrations, similar to the cytokine concentrations used by Dula *et al.* (10). Only the highest concentration of the cytokine mixture studied significantly decreased viability (~8.4%) after 24 h in mouse islets compared with untreated controls (Fig. 1*A*). Similar results were seen in human islets (~8.3% decrease in viability) ($p < 0.001$) (data not shown).

Similarly, glucose-stimulated insulin secretion was only affected by high levels of pro-inflammatory cytokines with a >70% decrease in insulin secretion with 0.1 and 1 RCC at 20 mM glucose compared with untreated controls (Fig. 1*B*). In contrast, disruption to $[Ca^{2+}]_i$ oscillation synchronization was observed at the lowest cytokine concentration used (Fig. 1, *C–F*); where synchronization decreased with increasing cytokine concentration compared with untreated controls (Fig. 1*G*). The peak $[Ca^{2+}]_i$ averaged over the islet also decreased significantly with 0.01, 0.1, and 1 RCC (Fig. 1*H*). This data confirms that $[Ca^{2+}]_i$ dynamics are disrupted with low levels of pro-inflammatory cytokines, under conditions where viability and levels of insulin release are maintained.

Pro-inflammatory Cytokines Decrease Cx36 Gap Junction Coupling in Mouse and Human Islets—Gap junction channels coordinate $[Ca^{2+}]_i$ dynamics. Therefore, given the disruption to $[Ca^{2+}]_i$ oscillation synchronization at low cytokine levels, we next quantified changes in Cx36 gap junction coupling with increasing cytokine levels. After 24 h in mouse islets, the 0.01, 0.1, and 1 RCC significantly decreased the average Cx36 gap junction coupling (Fig. 2, *A* and *B*), as measured by the fluorescence recovery rate. This decrease in gap junction coupling was accompanied by a decrease in the number of cells showing any fluorescence recovery (Fig. 2*C*), indicating a subset of cells showed a complete loss of gap junction coupling. After 24 h in human islets, all cytokine concentrations used decreased the average Cx36 gap junction coupling compared with untreated

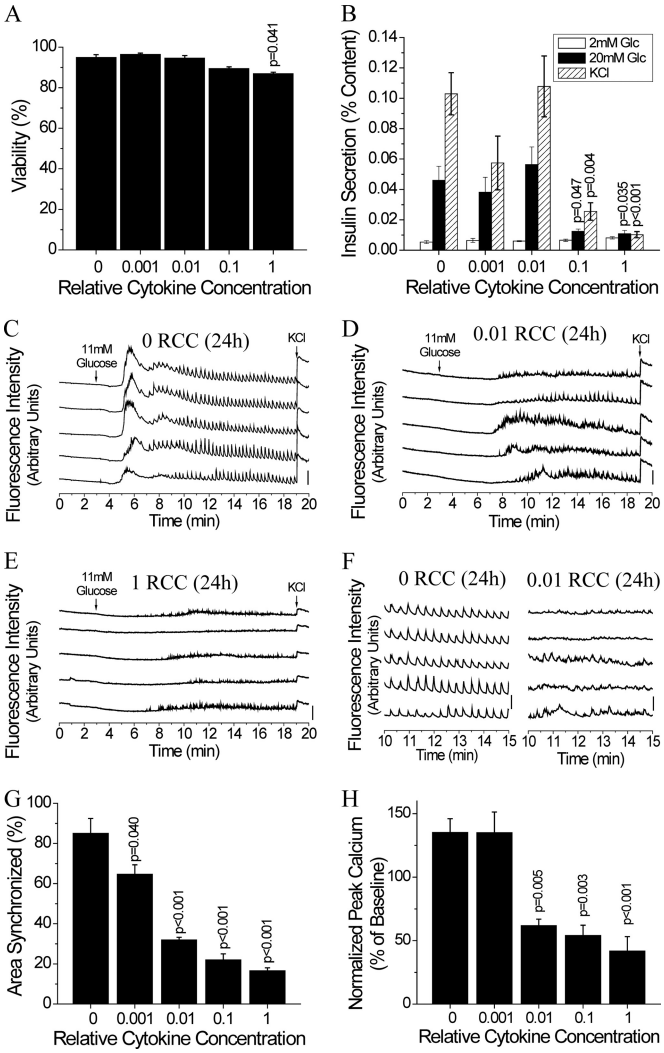

FIGURE 1. **Low level 24-h cytokine treatment disrupts $[Ca^{2+}]_i$ synchronization and dynamics.** *A,* percent viability in mouse islets after treatment for 24 h with increasing relative cytokine concentration. Data are averaged over islets from $n = 3$ mice. *B,* insulin secretion normalized to islet insulin content following cytokine treatment as in *A*, upon stimulation with glucose and/or 20 mM glucose with 20 mM KCl as indicated for 1 h. Data are averaged over islets from $n = 6$ mice. *C-E*, representative traces of $[Ca^{2+}]_i$, as defined by normalized Fluo-4 fluorescence intensity, from 2 mM glucose (0–3 min), to stimulation with 11 mM glucose (3–19 min), and stimulation with 20 mM glucose with 20 mM KCl (19–20 min), from 5 representative cells in 1 islet, treated with 0 (untreated) (*C*), 0.01 (*D*), or 1 (*E*) relative cytokine concentration, as in *A*. *Bars* indicate a 30% change in $[Ca^{2+}]_i$ compared with the baseline $[Ca^{2+}]_i$ levels. *F*, representative traces of $[Ca^{2+}]_i$, from *C* and *D*, enlarged over the 10–15 min period, over which % area synchronized and normalized peak calcium were quantified. *G,* relative area of the islet showing synchronized $[Ca^{2+}]_i$ oscillations following cytokine treatment as in *A*. Data averaged over islets from $n = 3$ mice. *H,* peak intracellular $[Ca^{2+}]_i$ levels normalized to baseline $[Ca^{2+}]_i$ following cytokine treatment as in *A*. Data averaged over islets from $n = 3$ mice. *Error bars* on all panels represent S.E. *p* values indicate significant differences compared with untreated controls (analysis of variance with Tukey's post hoc analysis, $\alpha = 0.05$).

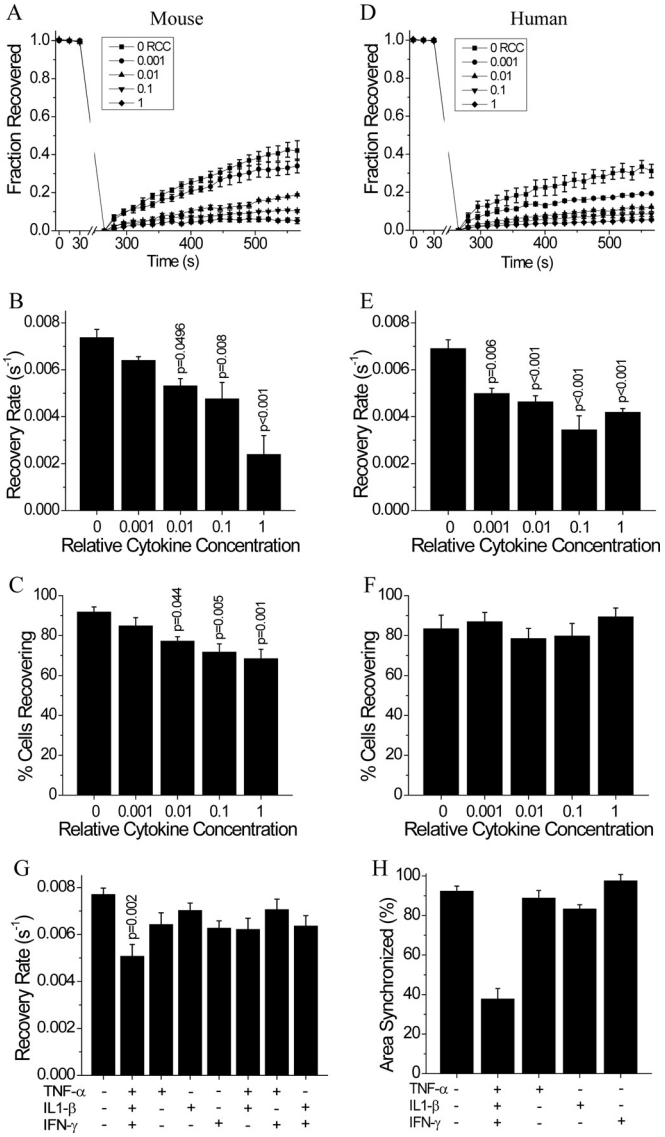

FIGURE 2. **Low level 24-h cytokine treatment disrupts gap junction coupling in mouse and human islets.** *A,* average fraction of fluorescence recovered over time, normalized to the average fluorescence before photobleaching; *B,* gap junction coupling, as measured by fluorescence recovery rate during FRAP; and *C,* percentage of cells with measurable levels of gap junction coupling, as defined by showing recovery of fluorescence during FRAP, in mouse islets following treatment for 24 h with increasing relative cytokine concentration. *D,* fraction of fluorescence recovered over time, normalized to the average fluorescence before photobleaching; *E,* gap junction coupling, as measured by fluorescence recovery rate during FRAP; and *F,* percentage of cells with measurable levels of gap junction coupling, as defined by showing recovery of fluorescence during FRAP, in human islets treated as in *A–C*. *G,* gap junction coupling in mouse islets following treatment for 24 h with individual, combinations of two, or all three cytokines at 0.1 relative cytokine concentration. *H,* relative area of the islet showing synchronized $[Ca^{2+}]_i$ oscillations following 24 h cytokine treatment with individual or a combination of all three cytokines at 0.1 relative cytokine concentration. Data in *A–C* and *G* are averaged over islets from $n = 5$ or 6 mice. Data in *H* are averaged over islets from $n = 2$ mice. Data in *D–F* are averaged over islets from $n = 4$ or 5 batches of islets from separate donors. *Error bars* on *panels A–G* represent S.E., whereas *error bars* on *panel H* represent standard deviation. *p* values indicate significant differences compared with untreated controls (analysis of variance with Tukey's post hoc analysis, $\alpha = 0.05$).

controls (Fig. 2, *D* and *E*), again as measured by the fluorescence recovery rate. In contrast to mouse islets, human islets showed no increase in the number of cells showing a complete loss of gap junction coupling under all cytokine concentrations used (Fig. 2*F*). This data shows that low levels of pro-inflammatory cytokines decrease gap junction coupling in both mouse and human islets; which in part, can explain the disruption to $[Ca^{2+}]_i$ oscillation synchronization and dynamics with low levels of cytokines.

To better understand the contributions of each individual cytokine to the observed decreases in coupling and $[Ca^{2+}]_i$ dynamics, islets were cultured for 24 h with 0.1 RCC of one, combinations of two, or all three cytokines, as compared with untreated controls. Individual or combinations of two cytokines had no significant effect on Cx36 gap junction coupling compared with untreated controls (Fig. 2*G*). Similarly, individual cytokines had no effect on $[Ca^{2+}]_i$ oscillation synchronization (Fig. 2*H*) and did not significantly decrease $[Ca^{2+}]_i$ peak. The combination of all three cytokines had the greatest effect on both coupling and $[Ca^{2+}]_i$ oscillation synchronization. This data supports the use of the cytokine mixture for use in investigating the mechanism of cytokine-induced islet dysfunction.

Islet Dysfunction after Acute Cytokine Treatment—Islet $[Ca^{2+}]_i$ dynamics and gap junction coupling were also analyzed after a 1-h treatment in mouse islets with increasing cytokine concentrations. Compared with untreated controls (Fig. 3*A*), $[Ca^{2+}]_i$ dynamics were significantly altered after 1-h treatments of 0.1 RCC (Fig. 3*B*) and 1 RCC (Fig. 3*C*). All cytokine concentrations decreased the $[Ca^{2+}]_i$ oscillation synchronization (Fig. 3*D*) and the peak intracellular calcium, averaged over the entire islet, was decreased by 0.1 and 1 RCC only (Fig. 3*E*). Similarly, Cx36 gap junction coupling was decreased by both the 0.1 and 1 RCC (Fig. 3*F*), whereas the number of cells showing no gap junction coupling was only significantly decreased at the 1 RCC (Fig. 3*G*).

To further investigate the mode of dysfunction over this short time period, acute treatment of islets with high levels of cytokines was studied. After elevating glucose to 11 mM, islets were treated with 0, 0.1, or 1 RCC as indicated in Fig. 4, *A–C*. $[Ca^{2+}]_i$ oscillations were disrupted within 30 min of 1 RCC treatment (Fig. 4*D*). Analysis of $[Ca^{2+}]_i$ oscillation synchronization and peak amplitude prior to and after cytokine treatment revealed that the $[Ca^{2+}]_i$ peak significantly decreased within 20 min for both 0.1 and 1 RCC (Fig. 4*E*). Oscillation synchronization decreased more slowly with 1 RCC showing significant decreases after 20 min (Fig. 4*F*) and 0.1 RCC showing significant decreases after 30 min.

This data shows that similar disruptions to $[Ca^{2+}]_i$ dynamics and gap junction coupling by pro-inflammatory cytokines also occur over acute treatments and suggests that the mechanism of regulation of Cx36 gap junction coupling occurs through fast mechanisms, such as channel gating or trafficking, rather than slower transcriptional changes.

PKCδ Modulates Cytokine-induced Changes in Cx36 Gap Junction Coupling—To investigate the role of PKCδ in modulating Cx36 function, we measured gap junction coupling after a 1-h treatment with 0.1 RCC, as this treatment level/time acutely decreased gap junction coupling and $[Ca^{2+}]_i$ dynamics. In mouse islets, 0.1 RCC treatment significantly decreased gap junction coupling compared with untreated control islets (Fig. 5*A*), as previously shown. Activation of PKCδ with PMA also decreased gap junction coupling, whereas inhibition of PKCδ

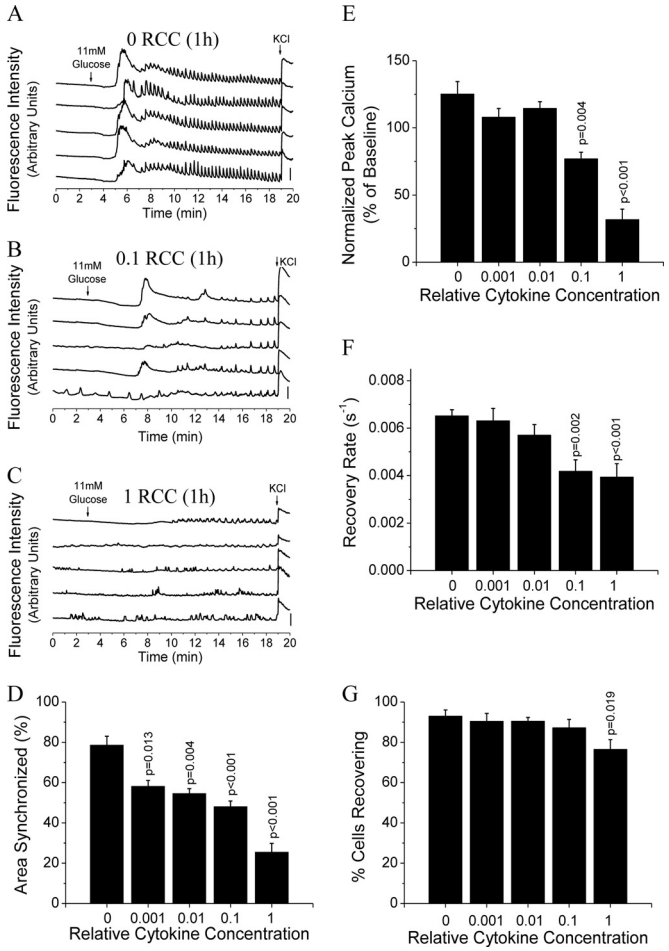

FIGURE 3. **1-h cytokine treatment disrupts $[Ca^{2+}]_i$ dynamics and gap junction coupling.** *A–C*, representative traces of $[Ca^{2+}]_i$, as defined by normalized Fluo-4 fluorescence intensity, from 2 mM glucose (0–3 min), to stimulation with 11 mM glucose (3–19 min), and stimulation with 20 mM glucose and 20 mM KCl (19–20 min), from 5 representative cells in 1 islet, treated with 0 (untreated) (*A*), 0.1 (*B*), or 1 (*C*) relative cytokine concentration for 1 h. *Bars* indicate a 30% change in $[Ca^{2+}]_i$ compared with the baseline $[Ca^{2+}]_i$ levels. *D*, relative area of the islet showing synchronized $[Ca^{2+}]_i$ oscillations following treatment for 1 h with increasing relative cytokine concentration. *E*, peak $[Ca^{2+}]_i$ levels normalized to baseline $[Ca^{2+}]_i$ following cytokine treatment as in *D*. Data in *D* and *E* are averaged over islets from $n = 3$ mice. *F*, gap junction coupling, as measured by fluorescence recovery rate during FRAP, following cytokine treatments as in *D*. *G*, percentage of cells with measurable levels of gap junction coupling, as defined by showing recovery of fluorescence during FRAP. Data in *F* and *G* are averaged over islets from $n = 6$ mice. *Error bars* on all panels represent S.E. *p* values indicate significant differences compared with untreated controls (analysis of variance with Tukey's post hoc analysis, $\alpha = 0.05$).

with rottlerin in the presence of 0.1 RCC recovered gap junction coupling to similar levels as those in untreated controls ($p = 0.42$) (Fig. 5, *A* and *B*). We also tested inhibition of all (α, β, γ, δ, and ϵ) PKC isoforms in mouse islets with 25 μM bisindolylmaleimide I for 24 h in the presence of 0.1 RCC treatment (44); however, this abolished gap junction coupling (data not shown, $n = 2$). Similar results upon PKCδ modulation were obtained with human islets (Fig. 5, *C* and *D*). Significant decreases in gap junction coupling were observed with both 0.1 RCC and PMA treatment, and PKCδ inhibition with rottlerin in conjunction with 0.1 RCC treatment led to recovery similar to untreated controls ($p = 0.52$). This data suggests that PKCδ regulates cytokine-induced decreases in Cx36 gap junction coupling.

NO Mediates Cytokine-induced Activation of PKCδ and Changes in Cx36 Gap Junction Coupling—Next we investigated the role of NO in mediating the effects of PKCδ on gap junction coupling. In mouse islets, 1 h culture with the NO donor molecules SNAP or DEANO decreased Cx36 gap junction coupling compared with untreated controls (Fig. 6*A*). Similar results were obtained in human islets with SNAP and DEANO treatments decreasing gap junction coupling compared with untreated controls (Fig. 6*B*). In both mouse and human islets, inhibition of PKCδ with rottlerin treatment in conjunction with either SNAP or DEANO recovered gap junction coupling to levels similar to untreated control islets (Fig. 6, *A* and *B*) ($p > 0.5$ for all). Treatment for 1 h with the NO synthase inhibitor L-NAME or the NO scavenging molecule cPTIO in mouse islets recovered gap junction coupling in the presence of 0.1 RCC, similar to levels in untreated controls ($p = 1.0$ and $p = 0.99$) (Fig. 6*C*). This data suggests a role for NO in activating PKCδ and mediating cytokine-induced changes in gap junction coupling.

To confirm that cytokine-induced NO production activates PKCδ, the amount of activated PKCδ was quantified using Western blot. Total activated (phosphorylated) PKCδ was detected at ~76 kDa and was normalized to α-tubulin (~55 kDa) for each sample after 24 h of culture with the indicated treatments (Fig. 6*D*). The relative amount of activated PKCδ increased with both low and high level cytokine concentrations (Fig. 6*E*). Treatment with the NO donor molecule SNAP increased activated PKCδ compared with untreated controls, whereas CIP treatment of this sample to remove all phosphate groups abolished activated PKCδ levels. Treatment with either the NOS inhibitor L-NAME or the NO scavenging molecule cPTIO in the presence of cytokine treatment led to similar PKCδ activation as untreated controls (Fig. 6*F*). This data confirms that the levels of NO produced in response to cytokine treatment activates PKCδ.

Pro-inflammatory Cytokines Decrease Membrane Cx36 and Alter Plaque Organization—To determine whether the observed decrease in Cx36 gap junction coupling after cytokine treatment was due to changes in membrane localization, Cx36 gap junction membrane and cytosolic protein were analyzed after 24- and 1-h treatments. Six individual Cx36 proteins form a connexin (hemi-channel), each ~36 kDa (45). Cx36 multimers were observed in isolated protein samples (Fig. 7). Although no bands were visible at ~36 kDa (Cx36 monomers), bands at ~75 kDa (dimers) and ~115 kDa (trimers) were observed and quantified. After 24 h treatment with 0.1 RCC, PKCδ activation with PMA, or increased NO with SNAP, Cx36 protein in the lysate supernatant, corresponding to cytosolic proteins, significantly increased compared with untreated controls (Fig. 7, *A* and *C*). Cx36 protein in the lysate pellet, corresponding to membrane protein, significantly decreased with 0.1 RCC, PMA, or SNAP treatments compared with untreated controls. After 1 h treatment, no significant change in Cx36 was observed in either the supernatant or pellet under all conditions (Fig. 7, *B* and *D*).

To further examine if changes in Cx36 gap junction plaque organization occur after cytokine treatment, plaque size and number were quantified in islet sections using immunofluores-

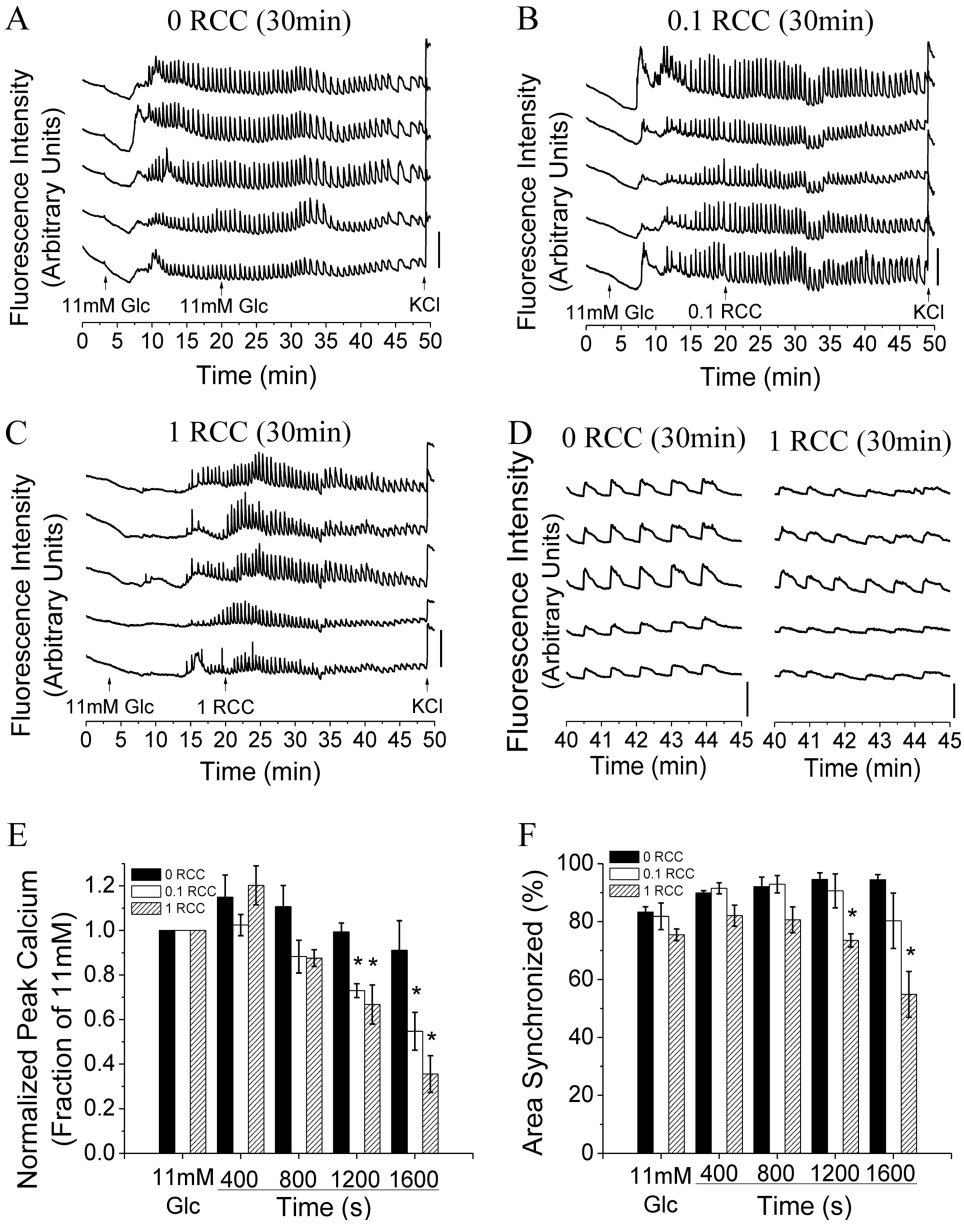

FIGURE 4. **Acute cytokine treatment disrupts $[Ca^{2+}]_i$ synchronization and dynamics.** *A–C*, representative traces of $[Ca^{2+}]_i$, as defined by normalized Fluo-4 fluorescence intensity, from 2 mM glucose (0–3 min), to stimulation with 11 mM glucose (3–20 min), plus either 11 mM glucose with 0, 0.1, or 1 relative cytokine concentration (20–49 min) and stimulation with 20 mM glucose and 20 mM KCl (49–50 min), from 5 representative cells in 1 islet. *Bars* indicate a 30% change in $[Ca^{2+}]_i$ compared with the baseline $[Ca^{2+}]_i$ levels. *D,* representative traces of $[Ca^{2+}]_i$, from *A* and *C*, enlarged over 40–45 min. *E,* peak intracellular $[Ca^{2+}]_i$ levels normalized to baseline $[Ca^{2+}]_i$ prior to and following acute cytokine treatment as in *E*. Data are averaged over islets from $n = 3$ mice. *F,* relative area of the islet showing synchronized $[Ca^{2+}]_i$ oscillations calculated for 400-s intervals prior to (11 mM) and following treatment with 0, 0.1, or 1 relative cytokine concentration. Data are averaged over islets from $n = 3$ mice. *Error bars* on all panels represent S.E. *, indicates a p value <0.05 compared with untreated controls (analysis of variance with Tukey's post hoc analysis, $\alpha = 0.05$).

cence (Fig. 8*A*). The membrane-localized plaque area per cell significantly decreased with increasing cytokine concentration after 24 h treatment (Fig. 8*B*). Similarly, 24 h treatment with PKCδ activation or increased NO decreased plaque area per cell compared with untreated controls (Fig. 8*C*). Islets treated for 1 h as in *B* and *C* did not show any significant changes in membrane-localized Cx36 (Fig. 8, *D* and *E*). Analysis of the relative distribution of plaque size revealed a small increase in plaques $<0.25\ \mu m^2$ with 0.1 RCC (Fig. 8*F*), whereas a decrease in large plaques $\geq 1.5\ \mu m^2$ was observed with 0.01 and 0.1 RCC (Fig. 8*G*). Treatment with PMA or SNAP for 24 h did not significantly affect the relative distribution of plaque size (Fig. 8*H*). No significant changes in relative plaque size distribution were observed with treatments over 1 h (data not shown). This data indicates that pro-inflammatory cytokines decrease gap junction coupling over 24 h, in part by decreasing plasma membrane levels of Cx36 and disrupting the organization of Cx36 gap junction plaques.

Discussion

Pro-inflammatory cytokines are mediators for the loss of islet function and mass in both T1D and T2D. *In vitro*, cytokine treatment has been shown to alter $[Ca^{2+}]_i$ dynamics, and this disruption is similar to that observed upon loss of gap junction

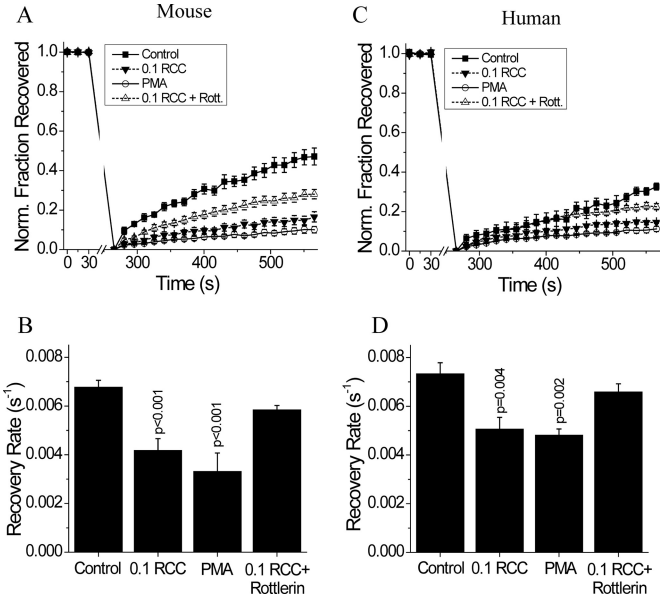

FIGURE 5. **PKCδ dependence of cytokine-mediated disruption of gap junctions in mouse and human islets.** *A,* average fraction of fluorescence recovered over time, normalized to the average fluorescence before photobleaching; and *B,* gap junction coupling, as measured by fluorescence recovery rate during FRAP, in mouse islets treated with 0.1 RCC, with 300 nM of the PKCδ activator PMA, or with 0.1 RCC plus 1 μM of the PKCδ inhibitor rottlerin, each for 1 h. Data are averaged over islets from $n = 6$ or 7 mice. *C,* fraction of fluorescence recovered over time, normalized to the average fluorescence before photobleaching; and *D,* gap junction coupling in human islets treated with 0.1 RCC and/or PKCδ modulators, as in *A*. Data are averaged over islets from $n = 5$ or 6 batches of islets from separate donors. *Error bars* on all panels represent S.E. *p* values indicate significant differences compared with untreated controls (analysis of variance with Tukey's post hoc analysis, $\alpha = 0.05$).

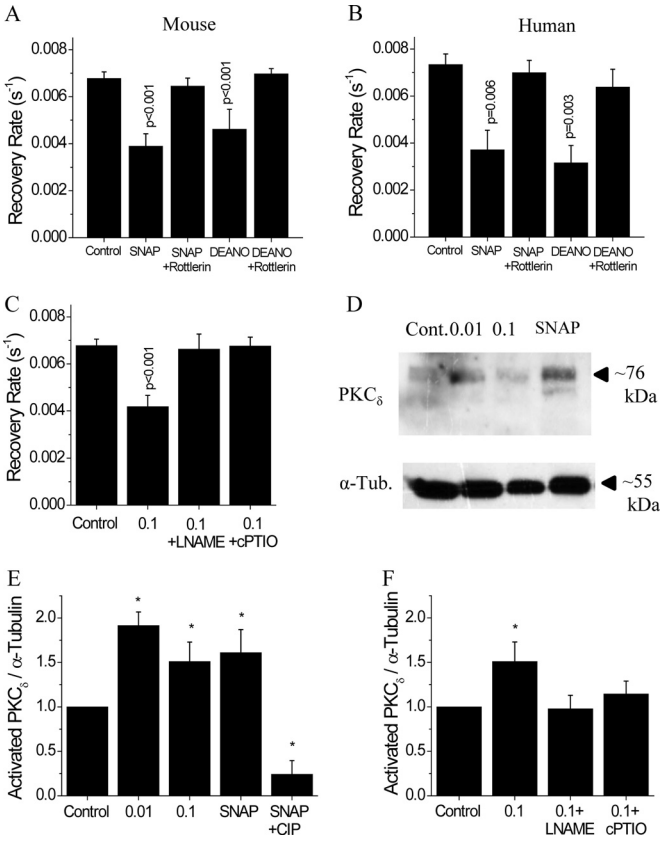

FIGURE 6. **PKCδ-mediated regulation of gap junction coupling in mouse and human islets.** *A,* gap junction coupling, as measured by fluorescence recovery rate during FRAP, in mouse islets treated with 5 mM of the NO donor SNAP, 5 mM SNAP with 1 μM of the PKCδ inhibitor rottlerin, 100 mM of the NO donor DEANO, or 100 mM DEANO with 1 μM rottlerin, each for 1 h. Data are averaged over islets from $n = 5$ or 6 mice. *B,* gap junction coupling in human islets treated with NO donors and PKCδ inhibitor, as in *A*. Data are averaged over islets from $n = 3$ or 5 batches of islets from separate donors. *C,* gap junction coupling in mouse islets treated with 0.1 RCC, 0.1 RCC with 1 mM of the NOS inhibitor L-NAME, or 0.1 RCC with 200 μM of the NO scavenger cPTIO, each for 1 h. Data are averaged over islets from $n = 6$ or 7 mice. *D,* representative Western blot; and *E,* quantification of activated (phosphorylated) PKCδ in samples from mouse islets treated for 24 h with 0 RCC, 0.01 RCC, 0.1 RCC, or 5 mM of the NO donor SNAP. As a negative control, protein from SNAP-treated islets was treated with CIP to dephosphorylate PKCδ. *F,* quantification of Western blots for activated PKCδ in samples from mouse islets treated for 24 h with 0 RCC, 0.1 RCC, 0.1 RCC plus 1 mM of the NOS inhibitor L-NAME, or 0.1 RCC plus 200 μM of the NO scavenger cPTIO. Each Western blot sample was also probed for α-tubulin on a separate blot. Activated PKCδ was normalized to α-tubulin for each sample. Normalized PKCδ of treated samples was then normalized to untreated control islets for each mouse. Data are averaged over islets from $n = 3$ mice. *Error bars* on all panels represent S.E. *, indicates a significant difference from untreated control islets based on a 95% confidence interval. *p* values indicate significant differences compared with untreated controls (analysis of variance with Tukey's post hoc analysis, $\alpha = 0.05$).

coupling. The goal of this study was to quantify changes in gap junction coupling and $[Ca^{2+}]_i$ with low levels of pro-inflammatory cytokines and understand the role of PKCδ in modulating cytokine-induced changes in gap junction coupling. As low level inflammation is present throughout diabetes development, understanding changes in $[Ca^{2+}]_i$ dynamics and gap junction coupling with pro-inflammatory cytokines will provide insight into islet dysfunction during the development of diabetes.

Low Levels of Pro-inflammatory Cytokines Disrupt $[Ca^{2+}]_i$ Dynamics and Cx36 Gap Junction Coupling—The cytokine mixture selected has been previously shown to alter $[Ca^{2+}]_i$ dynamics and insulin secretion in islets. We have not observed significant changes in coupling with this, or other combinations of the cytokines studied; therefore, the combination of all three cytokines was used to investigate the mechanisms of cytokine-induced dysfunction. This is supported by previous studies, which found greater disruption to $[Ca^{2+}]_i$ regulation in islets treated with a similar mixture of TNF-α, IL-1β, and IFN-γ, compared with treatment with individual cytokines (10).

The levels of pro-inflammatory cytokines investigated in this study had a minimal effect on islet viability, however, changes in islet function varied greatly over the range of cytokine concentrations studied. At high levels of pro-inflammatory cytokines, $[Ca^{2+}]_i$ dynamics were significantly interrupted and insulin secretion was inhibited, as has been previously shown (9, 10). However, at low levels of pro-inflammatory cytokines, where no changes in levels of insulin secretion were observed, altered $[Ca^{2+}]_i$ dynamics and decreased synchronization were still observed. This is similar to prior observations (10), which support that $[Ca^{2+}]_i$ dynamics are highly sensitive to disruption by pro-inflammatory cytokines. Disruptions to insulin dynamics have been shown with loss of Cx36 and altered $[Ca^{2+}]_i$ oscillation synchronization (18–20). Therefore, whereas the *levels* of insulin secretion under low levels of pro-inflammatory cytokine are conserved, the *dynamics* of release are likely disrupted. This would likely include loss of first phase and reduced pulsatile second phase, as observed upon loss of Cx36 (19, 20).

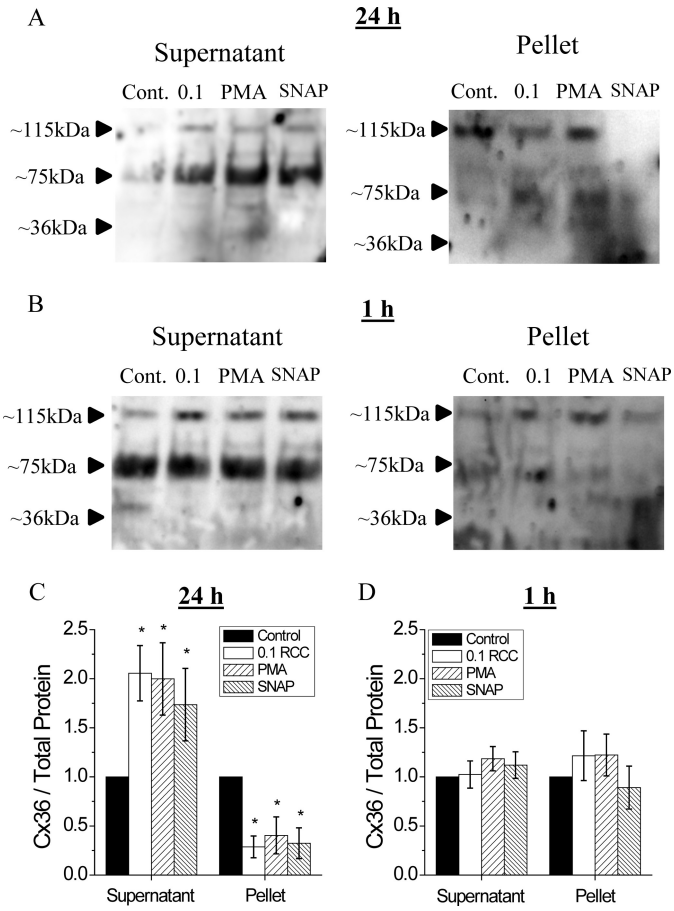

FIGURE 7. **PKCδ-mediated regulation of gap junction trafficking in mouse islets.** Representative Western blot of Cx36 protein in samples from mouse islets treated for 24 h (*A*) or 1 h (*B*) with 0 RCC, 0.1 RCC, 300 nM of the PKCδ activator PMA, or 5 mM of the NO donor SNAP. The protein was fractionated into supernatant (cytosolic protein) and pellet (membrane protein). Quantification of total Cx36 in islets treated for 24 (*C*) or 1 h (*D*) as described above. Total Cx36 content was measured as the sum of the 115- (trimer) and 75-kDa (dimer) bands for the supernatant and the 115-kDa (trimer) band only in the pellet. Total Cx36 was then normalized to untreated control islets for each mouse. Data are averaged over islets from $n = 3$ mice. *Error bars* on all panels represent S.E. *, indicates a significant difference from untreated control islets based on a 95% confidence interval.

Consistent with the observed disruptions to $[Ca^{2+}]_i$ dynamics, low levels of pro-inflammatory cytokines decreased Cx36 gap junction coupling in both mouse and human islets. This follows the well established role gap junctions play in synchronizing the oscillatory regulation of $[Ca^{2+}]_i$ (18, 20). In mouse islets, the decrease in average gap junction coupling (average recovery rate) was substantially greater than the decrease in the number of cells showing measurable gap junction coupling (% of cells showing recovery). This discrepancy suggests that gap junction coupling conductance between β-cells decreased in a highly variable manner, such that some cells are more susceptible to coupling decreases than others. The causes for this are unknown, but may be linked to variable susceptibility to cell death. For example, there exists heterogeneity in the mitochondrial membrane potential of individual β-cells (46) and this factor has been linked to susceptibility of β-cells to stress and apoptosis (47).

Human islets appeared to be more sensitive to disrupted gap junction coupling compared with mouse islets, showing decreases even at the lowest levels of pro-inflammatory cytokine tested. This may result from the use of mouse recombinant cytokines, which is consistent with previous studies that have shown an increased sensitivity of human islets to rat IL-1β and IFN-γ compared with rat islets (48). In further contrast to results in mouse islets, human islets only show a decrease in the average recovery rate, suggesting a more uniform disruption to gap junction coupling between β-cells. This may be due to spatial differences in cell-cell coupling and electrical activity between human and mouse islets. In human islets, clusters of β-cells can be physically separated by other endocrine cells, such as α-cells, whereas β-cells in mouse islets are generally coupled to each other in a single large cluster, with endocrine cells surrounding the cluster on the periphery (49). The differences in coupling architecture between species may therefore explain the differences in dose dependence and distribution of cytokine-mediated decreases in gap junction coupling, although this warrants further study.

Of note, gap junction coupling has been poorly characterized in human islets. We observed similar average recovery rates in untreated mouse and untreated human islets, indicating that similar levels of β-cell gap junction coupling are present in the two species. Given the importance of gap junctions to mouse islet function, this supports a similar importance for gap junctions in human islet function.

Dysregulation of Cx36 Gap Junction Coupling—Our results also indicate the mechanisms by which pro-inflammatory cytokines regulate Cx36 gap junction coupling (Fig. 9). Changes in gap junction plaque area per cell and plaque size were observed, including a relative decrease in the number of large ($\geq 1.5\ \mu m^2$) plaques. This suggests either a decrease in Cx36 trafficking *to* the membrane, an increase in trafficking *from* the membrane, or a reorganization of Cx36 channels in the membrane. Results from fractionation experiments further support altered Cx36 trafficking to or from the plasma membrane after long-term (24 h) treatment. Future studies measuring the dynamics of Cx36 turnover will be needed to further characterize this disruption. Previous measurements in INS-1E cells have also shown decreases in Cx36 gene expression, total protein, and Cx36 staining with similar levels of pro-inflammatory cytokines (30). Decreased Cx36 gene expression was also observed in islets with hyperglycemia and hyperlipidemia, conditions that produce high levels of pro-inflammatory cytokines (25, 26), and may represent an additional mechanism of Cx36 regulation. Further study is needed to determine the contributions of decreased Cx36 expression under the conditions studied here, including potential differences in sensitivity of cell lines *versus* primary mouse/human islets to cytokines.

We also observed significant disruptions to $[Ca^{2+}]_i$ dynamics and gap junction coupling between 30 min and 1 h of culture with pro-inflammatory cytokines. However, we did not observe changes in cytosolic and membrane localization of Cx36 or membrane organization of Cx36 gap junction plaques. This suggests that defects in trafficking are not occurring over acute (1 h) treatment times. Although rapid changes in $[Ca^{2+}]_i$ peak suggest a possible defect in $[Ca^{2+}]_i$ handling, the observed decrease in coupling after 30 min of cytokine treatment suggests that additional mechanisms of Cx36 regulation likely exist

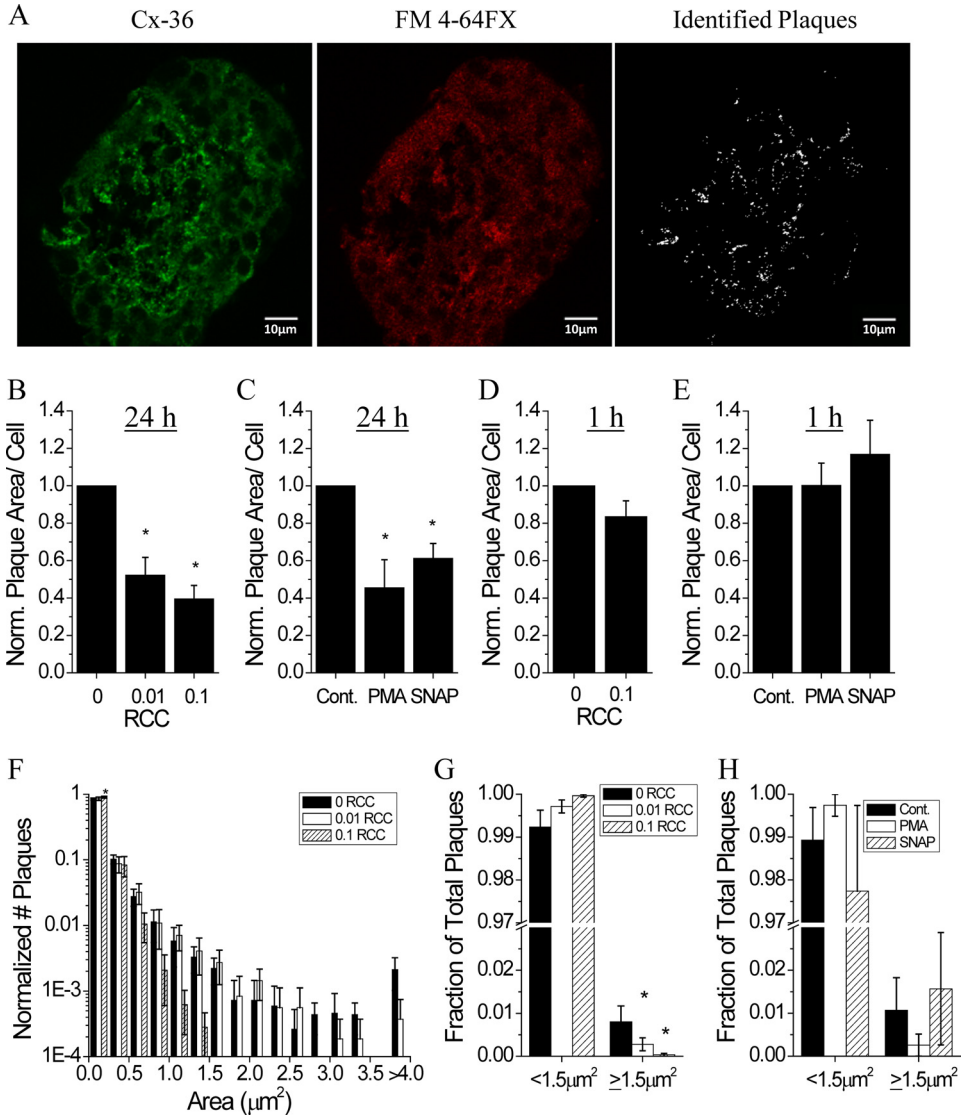

FIGURE 8. **Cytokine-mediated disruption to membrane-localized Cx36 gap junction plaques.** *A,* representative images of a mouse islet immunostained with Cx36, the fixable membrane stain FM 4-64FX, and the identified plaques used for analysis. Cx36 plaque area per cell following treatment with: *B,* 0, 0.01, or 0.1 RCC for 24 h; *C*, untreated, 300 nM of the PKCδ activator PMA, or 5 mM of the NO donor SNAP for 24 h; *D*, 0 or 0.1 RCC for 1 h; *E*, untreated, PMA, or SNAP for 1 h. Data are normalized to plaque area per cell measured in control islets for each mouse. *F,* histogram of Cx36 plaque areas for the indicated cytokine treatment. Data are normalized to the total number of plaques measured in control for each mouse. *G,* fraction of total plaques with an area $<1.5\ \mu m^2$ or $\geq 1.5\ \mu m^2$ after treatment with 0, 0.01, or 0.1 RCC for 24 h. *H,* fraction of total plaques with an area $<1.5\ \mu m^2$ or $\geq 1.5\ \mu m^2$ in untreated islets (*Cont.*) or islets treated with 300 mM PMA or 5 mM SNAP for 24 h. *, indicates a significant difference from control islets based on a 95% confidence interval. Data in *B–H* are averaged over islets from $n = 3–6$ mice. *Error bars* on all panels represent S.E.

that occur on a faster time scale than changes in gene expression or protein translation. Gating of Cx36 gap junction channels by phosphorylation of the connexin protein is a regulatory mechanism in AII amacrine cells to regulate Cx36 gap junction coupling (34). Thus altered channel gating may also mediate disruption to gap junction coupling resulting from pro-inflammatory cytokines.

NO Regulated PKCδ Modulates Cytokine-induced Changes in Cx36 Gap Junction Coupling—In the islet, pro-inflammatory cytokines have been shown to stimulate activation of the δ isoform of protein kinase C (PKCδ) (37). The observed decrease in gap junction coupling in both mouse and human islets upon activation of PKCδ with PMA and the recovery of coupling with the PKCδ inhibitor rottlerin upon cytokine treatment supports the hypothesis that PKCδ modulates cytokine-induced decreases in gap junction coupling. Although some studies have reported significant nonspecific effects with the use of rottlerin (50), the concentration used in this study was optimized for the minimal amount required to significantly recover gap junction coupling, which was ~10 times less than that reported. No other specific inhibitors of the δ isoform of PKC have been reported, and the abolished gap junction coupling upon inhibition of all isoforms of PKC suggests that other isoforms positively regulate coupling. Previous studies have shown activation of PKCδ with cytokine treatment (37): this is consistent with our data regarding activation of PKCδ and the role of PKCδ in regulating Cx36 gap junction coupling.

The mechanism of regulation of Cx36 by PKCδ still remains to be determined. We have shown that cytokines can regulate gap junction coupling over acute (1 h) time scales with NO and

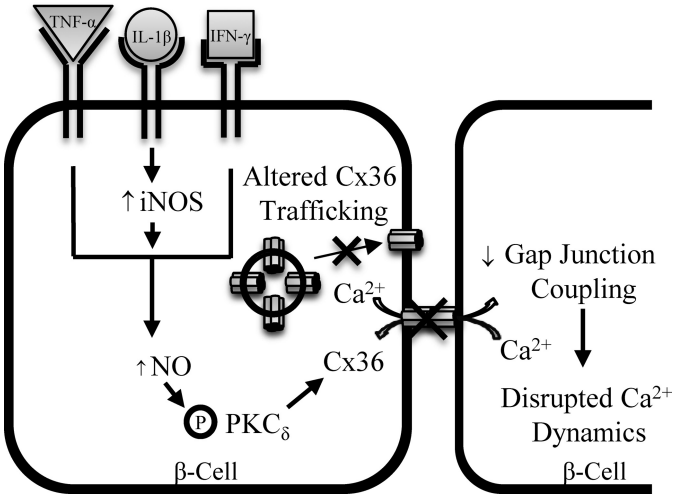

FIGURE 9. **Schematic representation of the proposed mechanism of cytokine-mediated decreases in Cx36 gap junction coupling.** Data indicate that cytokine-induced increases in NO via increased iNOS activity leads to activation of PKCδ. This leads to decreased Cx36 gap junction coupling, resulting in the observed disruption to $[Ca^{2+}]_i$ dynamics. Together with altered Cx36 trafficking and altered membrane plaque organization, this mechanism can explain the observed reduction in Cx36 gap junction coupling, and thus disruption to $[Ca^{2+}]_i$ dynamics and likely disruption to insulin secretion dynamics following pro-inflammatory cytokine treatment.

PKC_δ dependence. Because no changes in membrane Cx36 content or organization occurred over these time scales, this suggests that channel gating by phosphorylation is a potential regulatory mechanism. In rat epithelial cells, PKC phosphorylation of Cx43 regulates channel conductance (35) and PKCδ has been shown to directly phosphorylate Cx43 in fibroblasts (51), where the Cx36 C terminus contains similar serine residues that may be phosphorylated by PKCδ (52). Protein kinase A also regulates Cx36 in the retina through phosphorylation (34) and in the islet PKA has been shown to regulate GLP1-regulated synchronized $[Ca^{2+}]_i$ dynamics (53). However, the phosphorylation of Cx36 has not yet been studied in the islet.

Studies have suggested that localization of PKCδ to the cell membrane, such as with PMA treatment, can affect its action (54, 55). As this can occur over acute (~1 h) time scales, changes in PKCδ localization present an additional mechanism of cytokine and NO regulation of Cx36. However, determining the specific mode of action of PKCδ on Cx36 coupling is beyond the scope of this manuscript. Therefore future studies will be needed to precisely examine the role of PKCδ in regulating Cx36 gap junction coupling.

Cytokine treatment has also been shown to stimulate NO production in β-cells by activation of nitric-oxide synthase (NOS), which cleaves L-arginine to produce NO (11). Excessive levels of NO stimulated by pro-inflammatory cytokine have been shown to mediate cytokine-induced apoptosis and decrease insulin secretion (9, 56, 57). However, low basal levels of NO play a role in synchronizing glucose-induced $[Ca^{2+}]_i$ oscillations (58) and regulating insulin secretion (59). Although the role of NO in the islet is clearly diverse, the mechanisms by which NO mediates cytokine-induced islet dysfunction are not well understood. Previous studies have shown that NO activates PKCδ in cardiomyocytes (36) and as discussed above, our data strongly supports a role for NO in regulating Cx36 gap junction coupling through PKCδ in both mouse and human islets. Furthermore, our data has confirmed cytokine activation of PKCδ and suggests a role for NO in activating PKCδ. Cytokine activation of NOS may induce several parallel pathways causing islet dysfunction (60); however, inhibition of NOS activity (61) or scavenging of NO (62) confirmed the role of NO in directly activating PKC_δ.

Interestingly, whereas cytokines also caused a reorganization of Cx36 plaques on the cell membrane; specific activation of PKCδ or elevation of NO had little effect on relative membrane organization. This suggests that long-term exposure to cytokines may activate additional pathways that regulate Cx36 plaque organization. However, further study is needed to determine these potential mechanisms.

Overall, our data firmly supports the hypothesis that cytokine-induced decreases in gap junction coupling are mediated by NO-regulated PKCδ (Fig. 9) and includes changes to membrane Cx36 localization and function. As a result, $[Ca^{2+}]_i$ signaling is disrupted, which includes loss of synchronized $[Ca^{2+}]_i$ oscillations that likely disrupt insulin secretion dynamics.

Implications for Altered Gap Junction Coupling in Diabetes—Recent studies have indicated that Cx36 gap junction coupling is decreased in islets from high-fat diet fed mouse models of pre-diabetes (24). $[Ca^{2+}]_i$ dynamics are also disrupted in an ob/ob mouse model of obesity (63) consistent with a decrease in gap junction coupling (18). Furthermore, insulin secretion dynamics in humans with obesity (64), pre-diabetes (21), or T2D (65) are disrupted in a similar manner to disruption of dynamics following loss of Cx36. This similarity suggests that gap junctions are disrupted in the early stages of T2D and pre-diabetes, which coincides with the presence of low-levels of circulating pro-inflammatory cytokines (low-grade inflammation) that can occur in obesity following adipocyte stress (66). Our studies suggest that PKCδ regulation of gap junction coupling may underlie this disruption.

Recent studies have shown that Cx36 gap junctions can protect islets from cytokine or streptozotocin-induced cell death and oxidative stress (30, 31). Similarly, deletion of PKCδ in mice protects islets from cytokine-induced cell death (38), which is consistent with the mechanism we describe by which gap junctions are disrupted. Given the suggestion that decreases in Cx36 gap junction coupling occur in diabetes, the mechanisms we describe here may mediate this disruption to cause loss of protection against β-cell death and dysfunction. Thus altered gap junction coupling may be an underlying factor in disease development and progression. Further study is needed to determine the protective effects of Cx36 gap junction coupling and mechanisms involved in islet function. However, the mechanisms underlying dysfunction that we describe here may allow development of approaches to modulate gap junction coupling. This is particularly warranted given the current absence of robust and specific gap junction inhibitors/activators.

Conclusion—In summary, this study has determined that pro-inflammatory cytokines decrease Cx36 gap junction coupling through NO-regulated PKCδ-mediated decreases in Cx36 trafficking to or from the plasma membrane. High levels of pro-inflammatory cytokines caused cell death and decreased insulin secretion. Disrupted $[Ca^{2+}]_i$ dynamics and decreased

gap junction coupling were observed even with very low levels of cytokines and in the absence of disruptions to levels of insulin secretion (although dynamics of secretion are likely disrupted). Disruption to gap junction coupling over acute treatment times with NO and PKCδ dependence suggest additional mechanisms of Cx36 regulation. The discovery of these mechanisms will allow for understanding of disruptions to $[Ca^{2+}]_i$ regulation and the role of gap junction coupling underlying islet dysfunction in the development of diabetes.

Author Contributions—N. L. F. designed experiments, researched data, and wrote manuscript; R. L. W. researched data; A. H. researched data; M. J. W. researched data; R. K. P. B. designed experiments and edited the manuscript. All authors have read and approve of this manuscript.

Acknowledgments—We acknowledge the University of Colorado Anschutz Medical Campus Advanced Light Microscopy Core for assistance with imaging on the Zeiss LSM510 microscope, the Barbara Davis Center Islet Preparation Core for assistance with mouse islet isolations, and the Integrated Islet Distribution Program for providing isolated human islets. We thank Dr. Kurt Beam in the Department of Physiology and Biophysics, University of Colorado Denver, for use of his ultracentrifuge for protein fractionation experiments.

References

1. Robertson, R. P. (2009) β-Cell deterioration during diabetes: what's in the gun? *Trends Endocrinol. Metab.* **20,** 388–393
2. Imai, Y., Dobrian, A. D., Morris, M. A., and Nadler, J. L. (2013) Islet inflammation: a unifying target for diabetes treatment? *Trends Endocrinol. Metab.* **24,** 351–360
3. Padgett, L. E., Broniowska, K. A., Hansen, P. A., Corbett, J. A., and Tse, H. M. (2013) The role of reactive oxygen species and proinflammatory cytokines in type 1 diabetes pathogenesis. *Ann. N.Y. Acad. Sci.* **1281,** 16–35
4. Alexandraki, K., Piperi, C., Kalofoutis, C., Singh, J., Alaveras, A., and Kalofoutis, A. (2006) Inflammatory process in type 2 diabetes: the role of cytokines. *Ann. N.Y. Acad. Sci.* **1084,** 89–117
5. Akash, M. S., Rehman, K., and Chen, S. (2013) Role of inflammatory mechanisms in pathogenesis of type 2 diabetes. *J. Cell. Biochem.* **114,** 525–531
6. Cnop, M., Welsh, N., Jonas, J.-C., Jörns, A., Lenzen, S., and Eizirik, D. L. (2005) Mechanisms of pancreatic B-cell death in type 1 and type 2 diabetes: many differences, few similarities. *Diabetes* **54,** S97-S107
7. Donath, M. Y., and Shoelson, S. E. (2011) Type 2 diabetes as an inflammatory disease. *Nat. Rev. Immunol.* **11,** 98–107
8. Heitmeier, M. R., Scarim, A. L., and Corbett, J. A. (1997) Interferon-γ increases the sensitivity of islets of Langerhans for inducible nitric-oxide synthase expression induced by interleukin 1. *J. Biol. Chem.* **272,** 13697–13704
9. Corbett, J. A., Sweetland, M. A., Wang, J. L., Lancaster, J. R., Jr., and McDaniel, M. L. (1993) Nitric oxide mediates cytokine-induced inibition of insulin secretion by human islets of Langerhans. *Proc. Natl. Acad. Sci. U.S.A.* **90,** 1731–1735
10. Dula, S. B., Jecmenica, M., Wu, R., Jahanshahi, P., Verrilli, G. M., Carter, J. D., Brayman, K. L., and Nunemaker, C. S. (2010) Evidence that low-grade systemic inflammation can induce islet dysfunction as measured by impaired calcium handling. *Cell Calcium* **48,** 133–142
11. Corbett, J. A., Wang, J. L., Sweetland, M. A., Lancaster, J. R., Jr., and McDaniel, M. L. (1992) Interleukin 1β induces the formation of nitric oxide by β-cells purified from rodent islets of Langerhans. *J. Clin. Invest.* **90,** 2384–2391
12. Willmott, N. J., Galione, A., and Smith, P. A. (1995) Nitric oxide induces intracellular Ca^{2+} mobilization and increases secretion of incorporated 5-hydroxytryptamine in rat pancreatic β-cells. *FEBS Lett.* **371,** 99–104
13. Henquin, J. C., Ishiyama, N., Nenquin, M., Ravier, M. A., and Jonas, J.-C. (2002) Signals and pools underlying biphasic insulin secretion. *Diabetes* **51,** S60-S67
14. Matveyenko, A. V., Liuwantara, D., Gurlo, T., Kirakossian, D., Dalla Man, C., Cobelli, C., White, M. F., Copps, K. D., Volpi, E., Fujita, S., and Butler, P. C. (2012) Pulsatile portal vein insulin delivery enhances hepatic insulin action and signaling. *Diabetes* **61,** 2269–2279
15. Kono, T., Ahn, G., Moss, D. R., Gann, L., Zarain-Herzberg, A., Nishiki, Y., Fueger, P. T., Ogihara, T., and Evans-Molina, C. (2012) PPAR-γ activation restores pancreatic islet SERCA2 levels and prevents B-cell dysfunction under conditions of hyperglycemic and cytokine stress. *Mol. Endocrinol.* **26,** 257–271
16. Roe, M. W., Philipson, L. H., Frangakis, C. J., Kuznetsov, A., Mertz, R. J., Lancaster, M. E., Spencer, B., Worley, J. F., 3rd, and Dukes, I. D. (1994) Defective glucose-dependent endoplasmic reticulum Ca^{2+} sequestration in diabetic mouse islets of Langerhans. *J. Biol. Chem.* **269,** 18279–18282
17. Ramadan, J. W., Steiner, S. R., O'Neill, C. M., and Nunemaker, C. S. (2011) The central role of calcium in the effects of cytokines on beta-cell function: implications for type 1 and type 2 diabetes. *Cell Calcium* **50,** 481–490
18. Benninger, R. K., Zhang, M., Head, W. S., Satin, L. S., and Piston, D. W. (2008) Gap junction coupling and calcium waves in the pancreatic islet. *Biophys. J.* **95,** 5048–5061
19. Head, W. S., Orseth, M. L., Nunemaker, C. S., Satin, L. S., Piston, D. W., and Benninger, R. K. (2012) Connexin-36 gap junctions regulate *in vivo* first- and second-phase insulin secretion dynamics and glucose tolerance in the conscious mouse. *Diabetes* **61,** 1700–1707
20. Ravier, M. A., Güldenagel, M., Charollais, A., Gjinovci, A., Caille, D., Söhl, G., Wollheim, C. B., Willecke, K., Henquin, J.-C., and Meda, P. (2005) Loss of connexin36 channels alters β-cell coupling, islet synchronization of glucose-induced Ca^{2+} and insulin oscillations, and basal insulin release. *Diabetes* **54,** 1798–1807
21. Lo, S., Hawa, M., Beer, S. F., Pyke, D. A., and Leslie, R. D. (1992) Altered islet β-cell function before the onset of type 1 (insulin-dependent) diabetes mellitus. *Diabetologia* **35,** 277–282
22. Ize-Ludlow, D., Lightfoot, Y. L., Parker, M., Xue, S., Wasserfall, C., Haller, M. J., Schatz, D., Becker, D. J., Atkinson, M. A., and Mathews, C. E. (2011) Progressive erosion of β-cell function precedes the onset of hyperglycemia in the NOD mouse model of type 1 diabetes. *Diabetes* **60,** 2086–2091
23. O'Rahilly, S., Turner, R. C., and Matthews, D. R. (1988) Impaired pulsatile secretion of insulin in relatives of patients with non-insulin-dependent diabetes. *N. Engl. J. Med.* **318,** 1225–1230
24. Carvalho, C. P., Oliveira, R. B., Britan, A., Santos-Silva, J. C., Boschero, A. C., Meda, P., and Collares-Buzato, C. B. (2012) Impaired β-cell-β-cell coupling mediated by Cx36 gap junctions in prediabetic mice. *Am. J. Physiol. Endocrinol. Metab.* **303,** E144-E151
25. Haefliger, J.-A., Rohner-Jeanrenaud, F., Caille, D., Charollais, A., Meda, P., and Allagnat, F. (2013) Hyperglycemia downregulates Connexin36 in pancreatic islets via upregulation of ICER-1/ICER-1γ. *J. Mol. Endocrinol.* **51,** 49–58
26. Allagnat, F., Alonso, F., Martin, D., Abderrahmani, A., Waeber, G., and Haefliger, J. A. (2008) ICER-1γ overexpression drives palmitate-mediated connexin36 down-regulation in insulin-secreting cells. *J. Biol. Chem.* **283,** 5226–5234
27. Hodson, D. J., Mitchell, R. K., Bellomo, E. A., Sun, G., Vinet, L., Meda, P., Li, D., Li, W.-H., Bugliani, M., Marchetti, P., Bosco, D., Piemonti, L., Johnson, P., Hughes, S. J., and Rutter, G. A. (2013) Lipotoxicity disrupts incretin-regulated human β cell connectivity. *J. Clin. Invest.* **123,** 4182–4194
28. Böni-Schnetzler, M., Boller, S., Debray, S., Bouzakri, K., Meier, D. T., Prazak, R., Kerr-Conte, J., Pattou, F., Ehses, J. A., Schuit, F. C., and Donath, M. Y. (2009) Free fatty acids induce a proinflammatory response in islets via the abundantly expressed interleukin-1 receptor 1. *Endocrinology* **150,** 5218–5229
29. Maedler, K., Sergeev, P., Ris, F., Oberholzer, J., Joller-Jemelka, H. I., Spinas, G. A., Kaiser, N., Halban, P. A., and Donath, M. Y. (2002) Glucose-induced β cell production of IL-1β contributes to glucotoxicity in human pancreatic islets. *J. Clin. Invest.* **110,** 851–860
30. Allagnat, F., Klee, P., Cardozo, A. K., Meda, P., and Haefliger, J.-A. (2013) Connexin36 contributes to INS-1E cells survival through modulation of

cytokine-induced oxidative stress, ER stress and AMPK activity. *Cell Death Differ.* **20,** 1742–1752
31. Klee, P., Allagnat, F., Pontes, H., Cederroth, M., Charollais, A., Caille, D., Britan, A., Haefliger, J.-A., and Meda, P. (2011) Connexins protect mouse pancreatic β cells against apoptosis. *J. Clin. Invest.* **121,** 4870–4879
32. Farnsworth, N. L., and Benninger, R. K. (2014) New insights into the role of connexins in pancreatic islet function and diabetes. *FEBS Lett.* **588,** 1278–1287
33. Lampe, P. D., and Lau, A. F. (2000) Regulation of gap junctions by phosphorylation of connexins. *Arch. Biochem. Biophys.* **384,** 205–215
34. Urschel, S., Höher, T., Schubert, T., Alev, C., Söhl, G., Wörsdörfer, P., Asahara, T., Dermietzel, R., Weiler, R., and Willecke, K. (2006) Protein kinase A-mediated phosphorylation of connexin36 in mouse retina results in decreased gap junctional communication between AII amacrine cells. *J. Biol. Chem.* **281,** 33163–33171
35. Lampe, P. D., TenBroek, E. M., Burt, J. M., Kurata, W. E., Johnson, R. G., and Lau, A. F. (2000) Phosphorylation of connexin43 on serine 368 by protein kinase C regulates gap junctional communication. *J. Cell Biol.* **149,** 1503–1512
36. Yoshida, K., Mizukami, Y., and Kitakaze, M. (1999) Nitric oxide mediates protein kinase C isoform translocation in rat heart during postischemic reperfusion. *Biochim. Biophys. Acta* **1453,** 230–238
37. Carpenter, L., Cordery, D., and Biden, T. J. (2001) Protein kinase Cδ activation by interleukin-1β stabilizes inducible nitric-oxide synthase mRNA in pancreatic β-cells. *J. Biol. Chem.* **276,** 5368–5374
38. Cantley, J., Boslem, E., Laybutt, D. R., Cordery, D. V., Pearson, G., Carpenter, L., Leitges, M., and Biden, T. J. (2011) Deletion of protein kinase Cδ in mice modulates stability of inflammatory genes and protects against cytokine-stimulated beta cell death *in vitro* and *in vivo*. *Diabetologia* **54,** 380–389
39. Scharp, D. W., Kemp, C. B., Knight, M. J., Ballinger, W. F., and Lacy, P. E. (1973) Use of Ficoll in preparation of viable islets of Langerhans from rat pancreas. *Transplantation* **16,** 686–689
40. Koster, J. C., Remedi, M. S., Flagg, T. P., Johnson, J. D., Markova, K. P., Marshall, B. A., and Nichols, C. G. (2002) Hyperinsulinism induced by targeted suppression of β cell K-ATP channels. *Proc. Natl. Acad. Sci. U.S.A.* **99,** 16992–16997
41. Rocheleau, J. V., Remedi, M. S., Granada, B., Head, W. S., Koster, J. C., Nichols, C. G., and Piston, D. W. (2006) Critical role of gap junction coupled KATP channel activity for regulated insulin secretion. *PLos Biol.* **4,** e26
42. Hraha, T. H., Bernard, A. B., Nguyen, L. M., Anseth, K. S., and Benninger, R. K. (2014) Dimensionality and size scaling of coordinated Ca^{2+} dynamics in MIN6 β-cell clusters. *Biophys. J.* **106,** 299–309
43. Farnsworth, N. L., Hemmati, A., Pozzoli, M., and Benninger, R. K. (2014) Fluorescence recovery after photobleaching reveals regulation and distribution of connexin36 gap junction coupling within mouse islets of Langerhans. *J. Physiol.* **592,** 4431–4446
44. Toullec, D., Pianetti, P., Coste, H., Bellevergue, P., Grand-Perret, T., Ajakane, M., Baudet, V., Boissin, P., Boursier, E., Loriolle, F., Duhamel, L., Charon, D., and Kjrilovsky, J. (1991) The bisindolylmaleimide GF 109203X is a potent and selective inhbitor of protein kinase C*. *J. Biol. Chem.* **266,** 15771–15781
45. Perkins, G., Goodenough, D., and Sosinsky, G. (1997) Three-dimensional structure of the gap junction connexon. *Biophys. J.* **72,** 533–544
46. Wikstrom, J. D., Katzman, S. M., Mohamed, H., Twig, G., Graff, S. A., Heart, E., Molina, A. J. A., Corkey, B. E., and Shirihai, O. S. (2007) β-Cell mitochondria exhibit membrane potential heterogeneity that can be altered by stimulatory or toxic fuel levels. *Diabetes* **56,** 2569–2578
47. Molina, A. J., Wikstrom, J. D., Stiles, L., Las, G., Mohamed, H., Elorza, A., Walzer, G., Twig, G., Katz, S., Corkey, B. E., and Shirihai, O. S. (2009) Mitochondrial networking protects β-cells from nutrient-induced apoptosis. *Diabetes* **58,** 2303–2315
48. Kawahara, D. J., and Kenney, J. S. (1991) Species differences in human and rat islet sensitivity to human cytokines: monoclonal anti-interleukin-1 (IL-1) influences on direct and indirect IL-1-mediated islet effects. *Cytokine* **3,** 117–124
49. Cabrera, O., Berman, D. M., Kenyon, N. S., Ricordi, C., Berggren, P.-O., and Caicedo, A. (2006) The unique cytoarchitecture of human pancreatic islets has implications for islet cell function. *Proc. Natl. Acad. Sci. U.S.A.* **103,** 2334–2339
50. Soltoff, S. P. (2007) Rottlerin: an inappropriate and ineffective inhibitor of PKCδ. *Trends Pharmacol. Sci.* **28,** 453–458
51. Niger, C., Hebert, C., and Stains, J. P. (2010) Interaction of connexin43 and protein kinase C-δ during FGF2 signaling. *BMC Biochemistry* **11,** 14
52. Kothmann, W. W., Li, X., Burr, G. S., and O'Brien, J. (2007) Connexin35/36 is phosphorylated at regulatory sites in the retina. *Vis. Neurosci.* **24,** 363–375
53. Tsuboi, T., da Silva Xavier, G., Holz, G. G., Jouaville, L. S., Thomas, A. P., and Rutter, G. A. (2003) Glucagon-like peptide-1 mobilizes intracellular Ca^{2+} and stimulates mitochondrial ATP synthesis in pancreatic MIN6 β-cells. *Biochem. J.* **369,** 287–299
54. Hendey, B., Zhu, C. L., and Greenstein, S. (2002) Fas activation opposes PMA-stimulated changes in the localization of PKCd: a mechanism for reducing neutrophil adhesion to endothelial cells. *J. Leukoc. Biol.* **71,** 863–870
55. Mischak, H., Pierce, J. H., Goodnight, J., Kazanietz, M. G., Blumberg, P. M., and Mushinski, J. F. (1993) Phorbol ester-induced myeloid differentiation is mediated by protein kinase C-α and -δ and not by protein kinase C-βII, -ϵ, -ζ, and -η. *J. Biol. Chem.* **268,** 20110–20115
56. Kaneto, H., Fujii, J., Seo, H. G., Suzuki, K., Matsuoka, T., Nakamura, M., Tatsumi, H., Yamasaki, Y., Kamada, T., and Taniguchi, N. (1995) Apoptotic cell death triggered by nitric oxide in pancreatic β-cells. *Diabetes* **44,** 733–738
57. Thomas, H. E., Darwiche, R., Corbett, J. A., and Kay, T. W. (2002) Interleukin-1 plus γ-interferon-induced pancreatic β-cell dysfunction is mediated by β-cell nitric oxide production. *Diabetes* **51,** 311–316
58. Grapengiesser, E., Gylfe, E., Dansk, H., and Hellman, B. (2001) Nitric oxide induces synchronous Ca^{2+} transients in pancreatic β cells lacking contact. *Pancreas* **23,** 387–392
59. Eckersten, D., and Henningsson, R. (2012) Nitric oxide (NO): production and regulation of insulin secretion in islets of freely fed and fasted mice. *Regul. Pept.* **174,** 32–37
60. Eizirik, D. L., Sandler, S., Welsh, N., Cetkovic-Cvrlje, M., Nieman, A., Geller, D. A., Pipeleers, D. G., Bendtzen, K., and Hellerström, C. (1994) Cytokines suppress human islet function irrespective of their effects on nitric oxide generation. *J. Clin. Invest.* **93,** 1968–1974
61. Panagiotidis, G., Alm, P., and Lundquist, I. (1992) Inhibition of islet nitric-oxide synthase increases arginine-induced insulin release. *Eur. J. Pharmacol.* **229,** 277–278
62. Harada, N., Miura, T., Dairaku, Y., Kametani, R., Shibuya, M., Wang, R., Kawamura, S., and Matsuzaki, M. (2004) NO donor-activated PKC-δ plays a role in ischemic myocardial protection through accelerated opening of mitochondrial K-ATP channels. *J. Cardiovasc. Pharmacol.* **44,** 35–41
63. Ravier, M. A., Sehlin, J., and Henquin, J. C. (2002) Disorganization of cytoplasmic Ca^{2+} oscillations and pulsatile insulin secretion in islets from *ob/ob* mice. *Diabetologia* **45,** 1154–1163
64. Kanatsuka, A., Makino, H., Sakurada, M., Hashimoto, N., Iwaoka, H., Yamaguchi, T., Taira, M., Yoshida, S., and Yoshida, A. (1988) First-phase insulin response to glucose in nonobese or obese subjects with glucose intolerance: analysis by C-peptide secretion rate. *Metabolism* **37,** 878–884
65. Cerasi, E., and Luft, R. (1967) The plasma insulin response to glucose infusion in healthy subjects and in diabetes mellitus. *Acta Endocrinol.* **55,** 278–304
66. Verrilli, G. M., Corbin, K. L., and Nunemaker, C. S. (2011) Circulating cytokines as biomarkers for early stages of type 2 diabetes in the db/db mouse. *FASEB J.* **25,** 1063–1063